Overexpression of Mdm2 and MdmX Fusion Proteins Alters p53 Mediated Transactivation, Ubiquitination, and Degradation†

Mithua Ghosh, Keven Huang, and Steven J. Berberich*

Department of Biochemistry and Molecular Biology, Wright State University, Dayton, Ohio 45435

Received November 7, 2002; Revised Manuscript Received December 27, 2002

ABSTRACT: Mdm2 and MdmX function as cellular regulators of the p53 tumor suppressor protein. Mdm2, a p53 inducible protein, negatively regulates p53 by inhibiting p53 transcriptional activity and promoting ubiquitin mediated proteasome degradation. The Mdm2 ring finger domain has been shown to possess E3 ligase activity and to be a necessary domain for targeting p53 degradation. MdmX, a p53 binding protein sharing a high degree of structural homology with Mdm2, has emerged as another negative regulator of the p53 tumor suppressor. MdmX has also been shown to block p53 transactivation but unlike Mdm2 cannot induce p53 degradation. Since MdmX also possesses a ring finger domain that allows MdmX to associate with Mdm2, this study focused on elucidating how the ring and zinc fingers of these two proteins affected p53 function. We have generated a series of fusion proteins between Mdm2 and MdmX by swapping the ring finger domains with or without the zinc finger domains and examined how these fusions regulated p53 induced transactivation, ubiquitination, and degradation. All fusions inhibited the transcriptional activity of p53. In the absence of Mdm2, none of the fusion proteins could trigger p53 ubiquitination or degradation. However, in a cell line with endogenous Hdm2, Mdm2:X fusions containing the ring finger domain with or without the zinc finger domain demonstrated p53 ubiquitination presumably through stabilization of Hdm2. Additionally, an Mdm2:XZFRF fusion also degraded p53 when endogenous Hdm2 was present. Results from immunofluorescence studies suggest that p53 is colocalized to the cytoplasm when coexpressed with a Mdm2:X fusion (Mdm2:XZFRF) and that this fusion is capable of stabilizing endogenous Hdm2. Since none of the fusions triggered p53 ubiquitination in cells lacking Mdm2, these results indicate that the E3 ligase domain within the ring finger of Mdm2 when part of MdmX and the MdmX ring finger fused to Mdm2 were not sufficient to trigger p53 ubiquitination, in vivo.

The tumor suppressor gene *p53* is mutated in over 50% of human cancers (*1*). In nonstressed cells, p53 protein levels are relatively low due, in part, to its short half-life. However, p53 protein levels are increased in response to various types of DNA damage and cellular stresses (*2*). Stabilized p53 can result in either a G1/G2 cell cycle arrest or apoptosis-mediated cell death (*3*−*5*). Mdm2[1] and MdmX represent two important cellular regulators of p53. The *mdm2* gene was initially described as the second of three genes found amplified on murine double minute chromosomes isolated from a spontaneously transformed BALB/3T3 cell line (*6*). Mdm2, a transcriptional target of p53, is capable of binding to the N-terminal transactivation domain of p53 and inhibiting the transactivation and transrepression activities of p53 (*7*−*9*). Mdm2 is an ubiquitin (Ub) protein ligase (E3) for itself and p53 (*10*, *11*) and promotes rapid degradation of p53 through the ubiquitin proteolysis pathway (*12*−*14*). While endogenous levels of Mdm2 are sufficient to regulate p53 stability, the inappropriate overexpression of Mdm2 can reduce the levels of endogenous p53 (*15*) and in many cases represents a mechanism by which tumors eliminate p53. Consistent with that model, the human homologue of Mdm2, Hdm2, has been found amplified in approximately 7% of human tumors, many of which possess wild-type p53 (*16*).

MdmX, a p53 binding protein structurally homologous to Mdm2 (*17*), has emerged as another essential negative regulator of a p53 tumor suppressor since like Mdm2 (*18*, *19*), loss of MdmX expression results in p53 dependent embryonic lethality in mice (*20*−*22*). The region of highest homology between Mdm2 and MdmX is within the p53 binding domain in the amino terminus of MdmX (*23*). Both Mdm2 and MdmX show conservation within metal binding C-terminal ring finger motifs, which have been defined as a spatially conserved set of cysteine−histidine residues of the type C3HC4 (*17*, *24*). Despite the structural homology, genetic evidence suggests that *mdmx* cannot substitute for *mdm2* during early embryonic development. Unlike *mdm2*, *mdmx* gene expression is not modulated by DNA damage or p53 (*17*, *25*). MdmX does not target p53 for degradation and at elevated levels can even reverse Mdm2-mediated p53 degradation (*26*, *27*). MdmX not only stabilizes p53, but it is also capable of stabilizing Mdm2 by heterodimerizing with Mdm2 through its ring finger domain (*28*, *29*). Yeast two-hybrid analysis revealed that hetero-oligomerizaton between

† Supported by the NIH/NCI (CA66430 to S.J.B.). M.G. was supported by a WSU−SOM postdoctoral fellowship. K.H. was supported by the Biomedical Sciences Ph.D. program.

* Corresponding author. Phone: (937) 775-4494. Fax: (937) 775-3730. E-mail: steven.berberich@wright.edu.

[1] Abbreviations: mdm, murine double minute; hdm2, human homologue of mdm2; ZF, zinc finger; RF, ring finger; NLS, nuclear localization sequence; GFP, green fluorescent protein; PCR, polymerase chain reaction; TNT, in vitro transcription and translation.

10.1021/bi0271291 CCC: $25.00
Published on Web 02/06/2003

MdmX and Mdm2 was significantly more stable than homooligomerization of either protein (*28*).

The purpose of the present study was to investigate the function of different domains of Mdm2 and MdmX on p53 transactivation, ubiquitination, and degradation. Toward this end, fusion proteins were generated by swapping different domains between Mdm2 and MdmX. The results of this work revealed that all the Mdm2:X and MdmX:2 fusions inhibit the transcriptional activity of p53. In the absence of Mdm2, none of the fusions were able to trigger p53 ubiquitination or degradation. However, when the fusions were expressed in a cell line with endogenous Hdm2, the Mdm2:X fusions containing the ring finger domain with or without the zinc finger domain of MdmX demonstrated p53 ubiquitination. Additionally, the Mdm2:XZFRF fusion was found to degrade p53. Immunofluorescence studies showed that, when coexpressed with Mdm2:XZFRF, p53 was predominately localized to the cytoplasm, and coexpression of this fusion resulted in a significant stabilization of endogenous Hdm2. Taken together, these results suggest that the ring finger domain of MdmX present in both Mdm2:MdmX fusions seems to be sufficient to affect Mdm2 mediated ubiquitination of p53 through stabilization of endogenous Hdm2. In contrast, the E3 ligase domain within the ring finger of Mdm2, when part of the MdmX:Mdm2 fusions, was not sufficient to trigger p53 ubiquitination and degradation.

MATERIALS AND METHODS

Plasmids. The following plasmids used for the present study have been described previously: pcDNA3.1−mdm2, pcDNA3.1−mdmx, and pRChp53 (*25*, *26*, *30*). The synthetic Luciferase reporter plasmid pG13−Luciferase containing 13 copies of p53 consensus sequence was obtained by subcloning the promoter sequence from pG13CAT into pGL3Luc. The plasmid pEGFPN1 was purchased from Clontech. The His_6−ubiquitin expression plasmid was generously provided by Dr. Xirodimas from Dr. David Lane's laboratory. The Mdm2:X and MdmX:2 fusions were generated by PCR using *Pfx* DNA polymerase and fusion primers flanking the appropriate Mdm2 and MdmX ring and zinc finger regions. All fusion cDNA constructs (including stop codons) were cloned into pcDNA3.1V5/His (Invitrogen), such that the V5 epitope and six-histidine tag were not in frame with the cDNAs. The DNA sequence of each fusion cDNA was confirmed by DNA sequencing.

In Vitro Translation. Each fusion protein was initially confirmed by in vitro transcription and translation (TNT T7/T3 coupled Reticulocyte Lysate System; Promega). The in vitro translated proteins were radiolabeled with ^{35}S-methionine and resolved by SDS−PAGE. The fixed and dried gel was exposed to X-ray film for 24 h.

Cell Lines and Antibodies. H1299 cells, a non-small-cell lung carcinoma cell line devoid of p53, was purchased from the American Type Culture Collection. Mouse embryo fibroblast (MEF) 2KO cells, lacking both *p53* and *mdm2* genes were generously provided by Dr. Guillermina Lozano (MD Anderson). All cells were maintained in Dulbecco's modified Eagle medium (DMEM) supplemented with 10% fetal bovine serum and 10 μg of gentamicin per mL. p53 polyclonal antibody FL 1−393 (Santa Cruz Biotechnology, Inc.), monoclonal antibody Ab-6 (Oncogene), and monoclonal antibody Ab-1801 (Neomarkers) were used as indicated. The MdmX polyclonal rabbit antibody has been previously described (*25*). The monoclonal Mdm2 antibody 2A10 was a kind gift from Gerald Zambetti (St. Jude Research Hospital). Horseradish peroxidase-conjugated anti-mouse or anti-rabbit secondary antibodies (Promega) were combined with Super Signal substrate (Pierce) in the chemiluminescence detection of proteins. Cy2 and Texas Red conjugated to goat anti-rabbit and goat anti-mouse antibodies (Jackson Laboratories) were used in immunofluorescence experiments.

Transfections. H1299 (5.5×10^5/10 cm plate) and MEF 2KO cells (5×10^5/10 cm plate) were transiently transfected in serum and antibiotic free media with the indicated amount of plasmids using Lipofectamine (Invitrogen). After a 5 h incubation, the serum free media was replaced with DMEM containing serum and antibiotics. At 24 h post transfection cells were harvested, and whole cell extracts were prepared by incubating frozen cell pellets in a 2× volume of PBSA lysis buffer (phosphate-buffered saline [PBS] containing 5 mM EDTA and 0.5% Triton X-100). The pQE β-galactosidase reporter plasmid was included in all transfections to normalize for transfection efficiency. In p53 transactivation assays, the p53 reporter plasmid pG13Luc was included. Luciferase assays were performed as described by the manufacturer (Promega). The transactivation activity for each transfection condition was calculated as the relative luciferase units (average of two independent samples assayed in parallel) divided by the milliunits of β-galactosidase activity. Error bars represent the average deviation of the independent experiment.

Protein Analysis. For Western analyses, whole cell extracts based on equivalent β-galactosidase activity were resolved on a sodium dodecyl sulfate−10% polyacrylamide gel and subsequently transferred to a poly(vinylidene difluoride) membrane (Millipore) using a Transblot system (Bio-Rad). Imunoblotting was performed as described using appropriate primary antibodies at a 1:1000−1:5000 dilution and secondary antibodies (goat anti-mouse or goat anti-rabbit conjugated to horseradish peroxidase) at a 1:5000 dilution (*31*). Filters were then exposed to chemiluminescent reagent and subsequently exposed to X-ray film. To analyze for p53 ubiquitination, purification of His_6−ubiquitinated conjugates was performed as described by Xirodimas et al. (*32*).

Immunofluorescence Assay and Antibodies. For immunofluorescence assays, H1299 and 2KO were initially seeded onto four well chamber slides (LAB-TEK) at a concentration of ∼15 000 cells/well 1 day prior to transfection. After transfections, cells were fixed in PBS with 3% paraformaldehyde for 8 min at room temperature and subsequently permeabilized in PBS with 1% TritonX-100 solution for 20 min at room temperature. Cells were then blocked at 4 °C overnight in PBS solution containing 10% goat serum and 0.2% Tween-20. Primary antibodies were incubated for 1 h at room temperature at a dilution of 1:250−500, and the secondary antibody conjugated with either Texas Red or Cy2 (Jackson Laboratories) was incubated for 45 min at room temperature at a concentration of 1.0 μg/μL in 1:10 diluted blocking solution. Nuclei were stained with Hoechst dye 33342 (Sigma) in PBS at a concentration of 25 μg/mL for 5 min at room temperature and mounted in Gel mount (Biomeda Corp.). Between each antibody or stain addition,

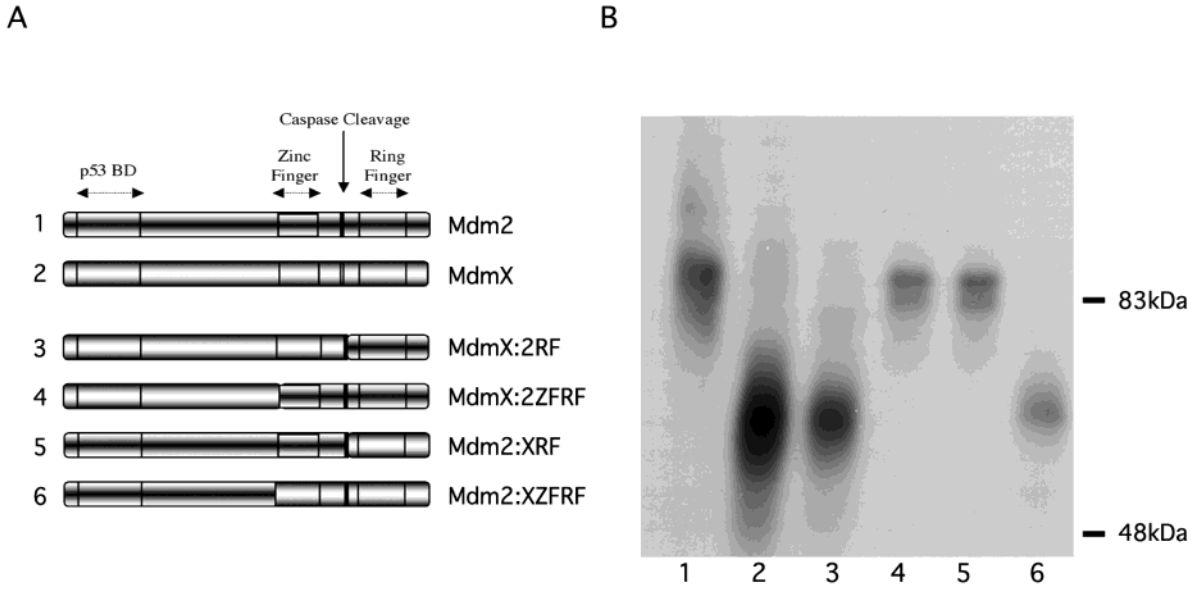

FIGURE 1: (A) Schematic of the Mdm2, MdmX, and fusion proteins. The location of the p53 binding domain (p53BD), ring, zinc, and caspase 3 cleavage sites are shown. All fusion cDNAs were sequenced to confirm proper reading frames. Mdm2:XRF contains Mdm2 amino acids 1−436 fused with MdmX amino acids 442−489. Mdm2:XZFRF contains Mdm2 amino acids 1−306 fused with MdmX amino acids 301−489. MdmX:2RF contains MdmX amino acids 1−441 fused with Mdm2 amino acids 437−489. MdmX:2ZFRF contains MdmX amino acids 1−299 fused with Mdm2 amino acids 294−489. (B) In vitro transcribed and translated Mdm2, MdmX, and fusion proteins were radiolabeled with ^{35}S-methionine and resolved by SDS−PAGE and autoradiography. Size markers are from NEN high molecular weight markers. Lane numbers correspond to the protein pictured in panel A.

the chambers were extensively washed 5 times with PBS. p53 was detected either with rabbit polyclonal FL 1−393 (Santa Cruz Biotechnology) or with mouse monoclonal p53 Ab-6 antibody (Oncogene Research Products). Mdm2 and Mdm2:XRF were detected with mouse monoclonal 2A10, and MdmX and the other fusions were detected with rabbit polyclonal MdmX antibody.

RESULTS

Characterization of Mdm2:X and MdmX:2 Fusion Proteins. Mdm2 and MdmX share a considerable degree of structural homology and have been characterized as negative regulators of the p53 tumor suppressor protein. However, while both proteins show conservation of C-terminal zinc and ring finger domains, only the Mdm2 ring finger has been reported to possess E3 ligase activity (*13*, *33*, *34*). To examine the functional similarities and differences between the zinc and the ring fingers of Mdm2 and MdmX, we generated a series of fusion proteins by swapping C-terminal regions of each protein. The fusions created in this study are shown schematically in Figure 1A. The MdmX:Mdm2 fusions were constructed by exchanging the ring finger domain with or without the zinc finger domain of MdmX with that of Mdm2 (MdmX:2ZFRF and MdmX:2RF). In the same way, the other Mdm2:MdmX hybrids were generated by replacing the ring finger domain with or without the zinc finger domain of Mdm2 with the analogous regions of MdmX (Mdm2:XZFRF and Mdm2:XRF). All constructs were generated by PCR cloning using *Pfx* DNA polymerase and subcloned into expression plasmids pcDNA3.1V5/His (including stop codons). The constructs were initially confirmed by DNA sequencing (data not shown), then transcribed and translated in vitro in the presence of [^{35}S]-methionine. The autoradiograph of in vitro translated proteins shown in Figure 1B shows that all four fusion constructs produced a protein in the range of 70−90 kDa. It is interesting to note that Mdm2:XRF migrated at a size consistent with a full-length Mdm2 (90 kDa) protein, whereas Mdm2:XZFRF, containing both the zinc and the ring finger of MdmX, migrated at approximately 70 kDa, the size reported for full-length MdmX. The fusion containing the Mdm2 zinc finger (MdmX:2ZFRF) also migrated at 90 kDa, suggesting that the region between the zinc and the ring finger domains of Mdm2 and MdmX affects the difference in migration between these proteins in SDS−PAGE.

Dose Dependent Effects of Fusion Proteins on p53 Transactivation and p53 Protein Stability. Both Mdm2 and MdmX have been shown to inhibit the transcriptional activity of p53 (*7*, *17*, *35*). Initially, we compared how the Mdm2:X and MdmX:2 fusion proteins affected p53 transactivation. H1299 cells, a non-small cell lung carcinoma cell line devoid of p53, were transfected with expression plasmids of human p53 alone or cotransfected with murine Mdm2, MdmX, or increasing concentrations of each of the four fusions (1:2−1:6). p53 mediated transactivation was monitored by inclusion of a reporter plasmid (pG13-Luciferase) containing 13 copies of a consensus p53 binding sequence. Consistent with earlier reports (*7*, *17*, *35*), both Mdm2 and MdmX were found to inhibit p53 mediated transactivation (Figure 2A, lanes 3 and 4). Coexpression of p53 with increasing concentrations of Mdm2:XZFRF (lanes 5−7), Mdm2:XRF (lanes 8−10), MdmX:2RF (lanes 11−13), and MdmX:2ZFRF (lanes 14−16) each resulted in a dose dependent decrease in transcriptional activity of p53. Interestingly, the p53 transcriptional repression was more dramatic with the Mdm2:X fusions as compared to the MdmX:2 fusions. Since Mdm2 and MdmX have different effects on p53 protein levels, we next wanted to determine if the differences on p53 transactivation by the fusions were the effect of alterations on p53 protein levels. In Figure 2A (lower panel),

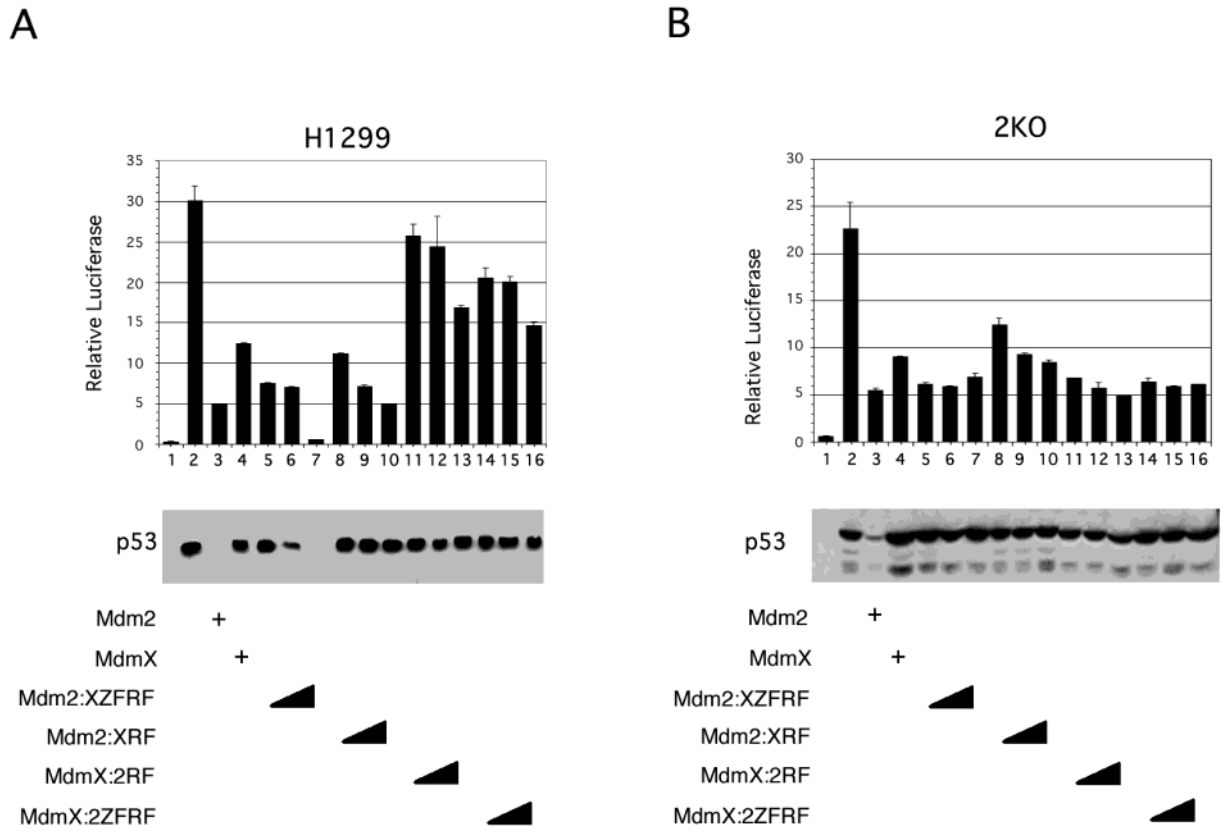

FIGURE 2: Dose dependent effects of Mdm2:X and MdmX:2 fusion proteins on transactivation and stabilization of p53. H1299 (A) and 2KO (B) cells were transfected with 500 ng (H1299) or 250 ng (2KO) of a hp53 expression vector either alone or with 3 μg of Mdm2, MdmX, or various increasing doses (1 μg, 2 μg, or 3 μg) of fusion protein expression vectors. A reporter plasmid (pG13LUC; 0.25−0.5 μg) was used to assess p53 mediated transactivation. pQE β-galactosidase and pEGFP plasmids were included in each transfection to normalize for transfection efficiency. Twenty-four hours after transfection, cells were harvested and assayed for β-galactosidase and luciferase activity. Luciferase activity ($\times 10^6$) was normalized to transfection efficiency. The *y* axis represents the relative luciferase activity (ratio of relative luciferase units per milliunit of β-galactosidase activity). Equivalent β-galactosidase units from each cell extract were resolved by SDS−PAGE, and p53 protein levels were detected by immunoblotting with a polyclonal p53 antibody. The results show that all the fusions inhibit the transcriptional activity of p53. The Mdm2:XZFRF fusion degraded p53 when transfected into H1299 but not in 2KO cells. Lane 1, vector; lane 2, p53 alone; lane 3, p53 with 3 μg of mdm2 plasmid; lane 4, p53 with 3 μg of mdmX plasmid; lanes 5−7, p53 with increasing amounts of mdm2:XZFRF plasmid; lanes 8−10, p53 with increasing amounts of mdm2:XRF plasmid; lanes 11−13, p53 with increasing amounts of mdmX:2RF plasmids; and lanes 14−16, p53 with increasing amounts of mdmX:2ZFRF plasmids. GFP western blots confirmed that the loading extracts based on β-galatosidase activity resulted in normalizing the extracts for transfection efficiency (data not shown).

Western blot analysis of p53 protein levels was performed after loading equivalent β-galactosidase units of protein extract from each of the transfections assayed in Figure 2A (upper panel). As previously reported (*26*, *33*, *36*), Mdm2 was found to target p53 for degradation, whereas MdmX was unable to elicit p53 degradation (Figure 2A, lower panel, lanes 3 and 4), even though p53 transactivation was inhibited upon coexpression with MdmX. In contrast to MdmX, the Mdm2:X fusion possessing the MdmX zinc and ring finger domains (Mdm2:XZFRF) was able to degrade p53 in a dose dependent manner (Figure 2A, lanes 5−7). While p53 degradation by Mdm2:XZFRF might explain the enhanced ability of this fusion to block p53 transactivation, a strong inhibition in p53 transactivation was also observed with Mdm2:XRF, a fusion that did not induce a decrease in p53 protein levels (Figure 2A, lanes 8−10). Additionally, neither of the MdmX:2 fusions (Figure 2A, lanes 11−16) affected p53 protein levels. Before concluding that the p53 degradation seen with Mdm2:XZFRF implied that the MdmX zinc and ring finger domains could substitute for the Mdm2 zinc and ring finger domains, we examined whether the p53 degradation observed with this fusion could occur in a cell line devoid of endogenous Mdm2. To do this, p53 transactivation and degradation was examined in mouse embryo fibroblasts devoid of p53 and Mdm2 (MEF 2KO). As in H1299 cells (Figure 2A), all the fusions were able to inhibit p53 mediated transactivation in a dose dependent manner in 2KO cells (Figure 2B). In contrast to H1299 cells, the p53 transactivation inhibition was more pronounced with MdmX:2 fusions in 2KO cells (Figure 2B, lanes 11−16). We are currently exploring whether this might be due to a difference in MdmX:2 stability in these two cell lines. However, when examining p53 degradation, we observed that none of the fusions had any detectable effect on p53 protein levels. The inability of Mdm2:XZFRF to degrade p53 in 2KO cells suggests that the Mdm2:X fusion was eliciting its effect on p53 stability through endogenous Hdm2. Nevertheless, all four fusions were able to inhibit the p53 mediated transactivation in both cell lines.

Mdm2:X Fusions Trigger p53 Ubiquitination in H1299 Cells. To further investigate the effects of the fusion proteins on p53 ubiquitination, an in vivo ubiquitination assay was performed (*32*). H1299 cells were transiently transfected with various p53, Mdm2, MdmX, and fusion expression plasmids.

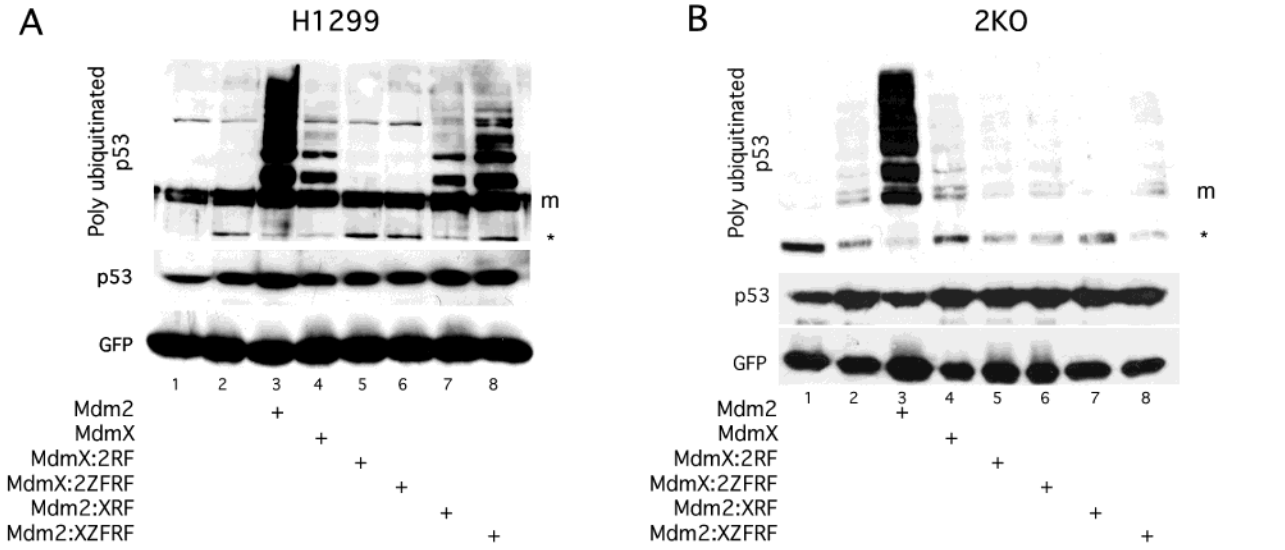

FIGURE 3: Mdm2:X and MdmX:2 fusions are unable to ubiquitinate p53 in cells devoid of Mdm2. In panel A (H1299) and B (2K0), cells were transfected with hp53 (1 μg) alone or with 2 μg of the indicated plasmids. Each transfection also contained a His-tagged ubiquitin and pEGFP expression vectors. Cells were untreated (lane 1) or treated 36 h post transfection with 20 μM MG132 for 4 h (lanes 2−8) prior to extract preparation and analysis as described in the Materials and Methods. Top panel: Nickel purified proteins probed for His-tagged p53 using p53 monoclonal antibodies. Middle panel: Total p53 protein levels were detected by Western blotting with monoclonal p53 antibody. Bottom panel: GFP protein levels detected by Western blotting of whole cell extracts. Asterisk (*) denotes position of unubiquitinated p53; m denotes position of mono-ubiquitinated p53.

Ubiquitination was assayed by including an expression vector for a His_6-tagged version of ubiquitin. Thirty-six hour post transfection cells were treated with 20 μM MG132, a 26S proteasome inhibitor, for 4 h. Transfection of p53 alone without MG132 treatment (Figure 3A, lane 1) and with MG132 treatment (Figure 3A, lane 2) showed mono-ubiquitinated p53, most likely the result of either endogenous Hdm2 or to an Mdm2-independent ubiquitinating activity. Cotransfection of p53 with Mdm2 resulted in an increase in p53 poly-ubiquitination represented by a ladder of p53 ubiquitinated forms (Figure 3A, lane 3). Coexpression of MdmX with p53 resulted in a more modest increase in ubiquitinated forms of p53 (Figure 3A, lane 4), likely resulting from the stabilization of endogenous Hdm2 (*37*). The MdmX:2 fusions demonstrated no detectable p53 ubiquitination above that seen with p53 alone (Figure 3A, lanes 5 and 6). Interestingly, the reciprocal chimeras (Mdm2:X) that had the ring finger with or without the zinc finger of MdmX fused to the N-terminus of Mdm2 were capable of inducing p53 ubiquitination in H1299 cells. It was also reproducibly observed that the overall level of poly-ubiquitinated forms of p53 was higher when p53 was cotransfected with Mdm2:XZFRF than with Mdm2:XRF (Figure 3A; compare lanes 7 and 8). Thus, the fusion Mdm2:XZFRF, which facilitated p53 degradation in H1299 cells (Figure 2A, lanes 5−7), also triggered an accumulation of multi- or poly-ubiquitinated p53 (Figure 3A, lane 8).

To investigate whether the ability of Mdm2:X fusions to trigger p53 ubiquitination required H(M)dm2, the in vivo ubiquitination assay was repeated in 2KO cells. As expected, coexpression of Mdm2 resulted in p53 poly-ubiquitination (Figure 3B, lane 3), while MdmX was not capable of inducing any p53 ubiquitination above that observed with p53 alone (Figure 3B, lane 4). These findings reconfirm that MdmX by itself does not have ubiquitin ligase activity toward p53 (*37*). Similarly, none of the fusions resulted in accumulation of ubiquitinated forms of p53 (Figure 3B, lanes 5−8). The results suggest that neither the substitution of the Mdm2 zinc and or ring fingers for MdmX nor the reverse fusions were able to ubiquitinate or degrade p53 in a cell line lacking Mdm2. However, in a cell line possessing endogenous Hdm2 (H1299), the substitution of the MdmX ring (RF) or zinc and ring (ZFRF) finger domains resulted in fusions with the capacity to trigger an Hdm2 dependent p53 ubiquitination, and in the case of the Mdm2:XZFRF, p53 degradation.

Cellular Localization of p53 in the Presence of the Mdm2:X and MdmX:2 Fusions. To address how the fusions demonstrated differing effects on p53 ubiquitination and degradation, we next investigated whether the coexpression of p53 with the various fusions affected p53 subcellular localization. H1299 and 2KO cells were transfected with plasmids encoding p53 alone or with Mdm2, MdmX, Mdm2:X, and MdmX:2 fusions, and p53 cellular localization was examined as described in the Materials and Methods. When p53 was transfected alone, the majority of p53 transfected cells showed an exclusively nuclear p53 staining pattern (Figure 4A,B). Cells overexpressing both Mdm2 and p53 demonstrated a strong nuclear/weak cytoplasmic p53 staining, whereas Mdm2 localization was exclusively nuclear (Figure 4A,B). Coexpression of MdmX with p53 resulted in p53 being localized to both the nucleus and the cytoplasm with MdmX being predominately cytoplasmic, although nuclear staining was clearly detected (Figure 4A,B upper and middle panels). Cotransfection of p53 with the MdmX:2 fusions (MdmX:2RF and MdmX:2ZFRF) and Mdm2:XRF all produced strong nuclear and weak cytoplasmic staining of p53. Each of these fusions was also localized predominantly in the nucleus (Figure 4A,B upper and middle panels). Interestingly in H1299 cells expressing the Mdm2:XZFRF fusion, p53 was localized in both the nucleus and the cytoplasm with Mdm2:XZFRF showing strong cytoplasmic staining (Figure 4A). The ability of Mdm2:XZFRF to induce a cytoplasmic localization of p53 was not observed when

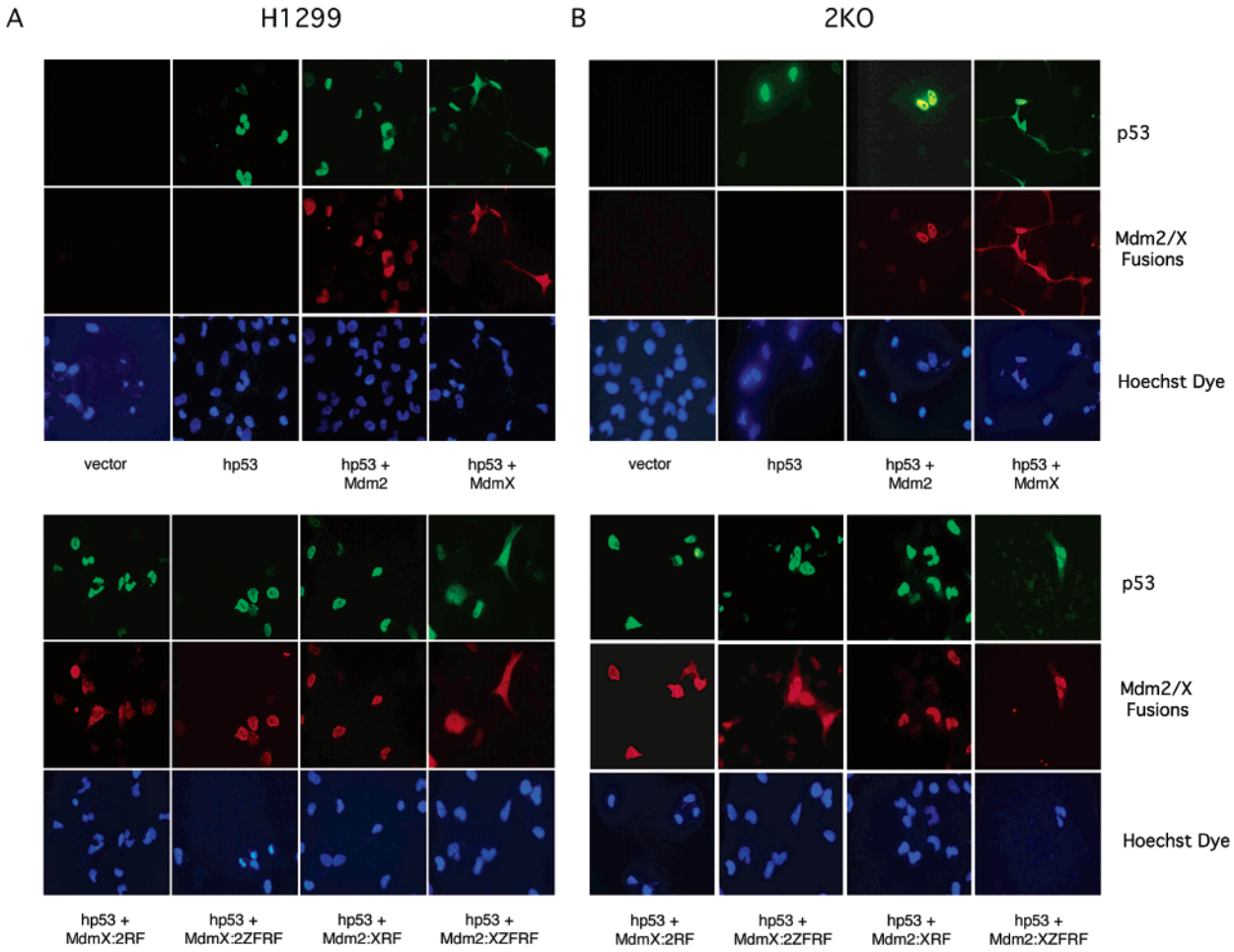

FIGURE 4: Cellular localization of p53 when coexpressed with Mdm2, MdmX, or the fusion proteins. (A) H1299 and (B) 2KO cells were transfected with expression vectors encoding p53 alone or with Mdm2, MdmX, or the indicated fusions. p53 localization was detected using p53 polyclonal or monoclonal antibodies and the appropriate secondary antibody conjugated with Cy2 (green panels). Mdm2, MdmX, or the fusion proteins were detected with the appropriate Mdm2 or MdmX antibodies and a secondary antibody conjugated with Texas Red (red panels). Nuclei were stained with Hoechst dye (blue panels). The fusion Mdm2:XZFRF itself is localized to the cytoplasm in contrast to the other fusions that are predominantly in the nucleus.

the proteins were expressed in 2KO cells (Figure 4B). From this, we conclude that Mdm2:XZFRF alters p53 localization through endogenous Hdm2.

Mdm2:XZFRF Fusion Stabilizes Endogenous Hdm2. Last, to directly demonstrate that the Mdm2:XZFRF was affecting the stability of Hdm2 in H1299 cells, we performed immunofluorescence experiments in H1299 cells to examine if the fusions with the MdmX C-terminal domains could stabilize endogenous Hdm2. We first determined which specific antibodies could be used to separately detect endogenous Hdm2 and the various fusions. In data not shown, the 2A10 Mdm2 monoclonal antibody was shown to be specific for endogenous Hdm2 and not capable of crossreacting with any of the fusions examined. Additionally, our MdmX polyclonal antibody was able to detect the MdmX:2 fusions (MdmX:2RF and MdmX:2ZFRF) and Mdm2:XZFRF fusions and did not detect the endogenous Hdm2.

We subsequently carried out immunofluorescence experiments in H1299 cells, monitoring transfected cells for either p53 (Figure 5A, lane b), fusions (Figure 5A), or endogenous Hdm2 (Figure 5A, lanes g−l) protein. On the basis of analyzing approximately 50 transfected cells per condition, 43% of the H1299 cells expressing p53 also possessed elevated Hdm2 protein (Figure 5B), a result consistent with previous findings that Mdm2 is one of the transcriptional targets of p53. Cotransfection of MdmX:2 fusions (MdmX:2RF and MdmX:2ZFRF) with p53 resulted in only 20 and 12%, respectively, of the transfected cells showing increases in the levels of endogenous Hdm2 (Figure 5B). It is possible that the decrease in Hdm2 resulted from the inhibition of p53 transactivation caused by overexpression of these fusions. Interestingly, when the fusion Mdm2:XZFRF, which was found to inhibit p53 mediated transactivation and increase p53 degradation, was coexpressed with p53, it resulted in a stabilization of Hdm2 in 72% of the transfected cells analyzed (Figure 5B). To confirm that the effects of the fusion on Hdm2 stabilization were not simply alterations of p53 transactivation, the experiment was repeated by expressing only the fusions in H1299 cells. Again, the MdmX:2 fusions were unable to stabilize Hdm2 (Figure 5C) while the Mdm2:XZFRF fusion, even in absence of p53, was able to stabilize Hdm2 (Figure 5C) albeit to lower levels than seen when the fusion was cotransfected with p53 (Figure 5B). Both immunofluorescence approaches confirm our hypothesis that the MdmX carboxyl ring and zinc finger domains fused to the N-terminus of Mdm2 can stabilize endogenous Hdm2. This effect leads to ubiquitination and

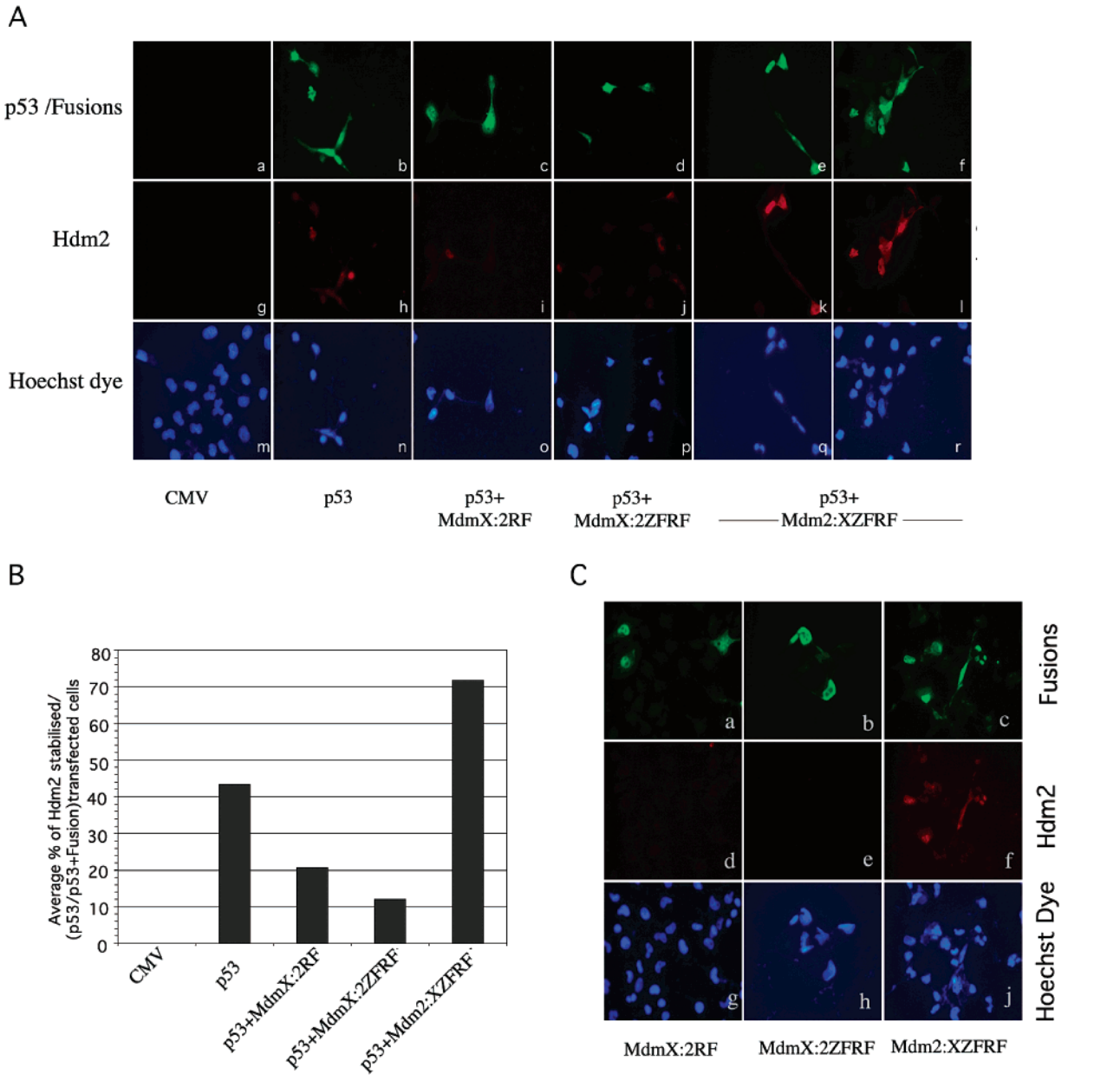

FIGURE 5: Stabilization of Hdm2 by Mdm2:XZFRF. (A) H1299 cells were transfected with the indicated plasmids and then examined by immunofluorescence for Hdm2 (lanes g−l) using 2A10 antibody, which does not react with any of the indicated fusion proteins (data not shown). p53 (lane b) or the various fusions were also monitored (c−f). Nuclei (lanes m−r) were stained with Hoechst dye. (B) The localization of Hdm2 in at least 50 transfected cells were counted. The percentage of Hdm2 positive cells showing signal above the level detected in untransfected cells was plotted as a percentage of the total number of p53 or fusion positive cells. (C) H1299 cells were transfected with the indicated fusion. As when cotransfected with p53, Mdm2:XZFRF was able to stablize endogenous Hdm2.

degradation of p53. These results suggest a possible role for the MdmX carboxyl terminal domain on the p53−Mdm2 autoregulatory feedback loop.

DISCUSSION

On the basis of the embryonic lethality observed in mice lacking either *mdm2* or *mdmX*, it appears that the proteins encoded by these genes represent important cellular regulators of p53, at least during the early stages of mouse development (*18*−*22*). Surprisingly, the embryonic lethality observed, while clearly p53 dependent, occurs at genetically distinct developmental points. This difference may result from either differences in the developmental expression of Mdm2 and MdmX or may be based on the fact that these two proteins possess unique mechanisms for regulating p53 activity. Upon Mdm2 activation, p53 transactivation is repressed, and p53 protein levels are reduced. In contrast, we and others have demonstrated that MdmX overexpression can only repress p53 transactivation although under certain conditions, MdmX is capable of reversing Mdm2 mediated p53 degradation (*26*, *27*, *29*). Recently, several laboratories have put forward models to address both the inability of MdmX to degrade p53 and the role of MdmX in regulating Mdm2 mediated degradation of p53. Stad et al. recently reported that while MdmX was unable to function in ubiquitinating p53, it could stimulate the ability of endogenous Mdm2 to induce p53 ubiquitination (*37*). The results in the present study are consistent with that finding as MdmX, while unable to trigger p53 ubiquitination in 2KO cells (Figure 3B), was able to induce a modest level of p53

ubiqutination in H1299 cells that possess Hdm2 (Figure 3A). Interestingly, this level of multi- or poly-ubiquitination was unable to induce p53 degradation (Figure 2A, lane 4) consistent with another report that poly-ubiquitinated rather than mono- or di-ubiquitinated proteins are efficiently recognized and degraded by the proteasomes (*38*).

To test whether the inability of MdmX to degrade p53 was the result of an inactive E3 ligase activity within the MdmX ring finger domain, we tested four fusions that were reciprocal exchanges of the ring finger and the zinc and ring finger domains of Mdm2 and MdmX. To our initial surprise, none of the fusions were able to degrade or ubiquitinate p53 in cells lacking Mdm2 (Figure 3B). It appears that the Mdm2 ring finger, with or without the zinc finger, cannot function as an E3 ligase when fused to a N-terminal MdmX protein. This conclusion is supported by the results of Argentini et al., which suggested that the central region of Mdm2 (AA 222−272) was necessary for efficient and effective ubiquitination and degradatation of p53 (*39*). However, when that domain of Mdm2 was fused with either the MdmX zinc and ring finger domains or the MdmX ring finger domain, neither fusion was able to elicit p53 ubiquitination in the absence of Mdm2 (Figure 3B), providing further evidence that the MdmX C-terminal domain does not possess a functional E3 ligase.

While none of the fusions were capable of eliciting an Mdm2-like p53 ubiqutination, all four fusions were able to block p53 transactivation (Figure 2). In cells devoid of Mdm2, each fusion showed a comparable, dose dependent inhibition of p53 transactivation (Figure 2B). These findings are consistent with the observation that, in the absence of p53 degradation, the Mdm2 and MdmX p53 binding domains show nearly equivalent binding affinities to p53 (*40*). In H1299 cells, the p53 transcriptional inhibition by the Mdm2:X fusions (Figure 2A, lanes 5−10) was significantly more pronounced than the inhibition observed with the MdmX:2 fusions (Figure 2A, lanes 11−16). Since both Mdm2:X fusions blocked p53 transactivation but only Mdm2:XZFRF was able to trigger p53 degradation in H1299 cells (Figure 2A, lanes 5−8), it appears that degradation of p53 protein cannot completely explain the enhanced p53 transcriptional inhibition seen with these Mdm2:X fusions.

One potential explanation as to why the Mdm2:X fusions were more effective in blocking p53 transactivation in H1299 cells was obtained when we examined how all four fusions affected p53 ubiquitination. In the p53 ubiquitination experiments, both Mdm2:X fusions induced a p53 ubiquitination activity in H1299 cells (Figure 3A vs 3B). Given the reports that p53 ubiquitination may disrupt the p53 tetramer (*41*−*43*), it is plausible that the enhanced p53 transcriptional repression observed with the Mdm2:X fusions might result from a breakdown of transcriptionally active p53 tetramers. To test whether the enhanced ubiquitination was causing p53 relocalization to the cytoplasm thereby affecting p53 transactivation, we examined the localization of p53 in cells overexpressing the various MdmX:2 and Mdm2:X fusions (Figure 4). In H1299 cells, MdmX (Figure 4, lanes 3) and Mdm2:XZFRF (Figure 4, lanes 8) were both cytoplasmic and nuclear localized and resulted in modest (MdmX) to dramatic (Mdm2:XZFRF) cytoplasmic localization of p53. In contrast, Mdm2:XRF (Figure 4A, lane 7) failed to alter p53 localization suggesting that increased p53 ubiquitination does not necessarily equate with an increase in cytoplasmically localized p53.

With respect to the role of MdmX in Mdm2-mediated p53 degradation, it has been proposed that MdmX, at low levels, is required for Mdm2 mediated degradation of p53 implying that the Mdm2:MdmX heterodimer is an essential component for p53 degradation (*44*). Furthermore they report, as have others, that MdmX is exclusively cytoplasmic, unless coexpressed with Mdm2 (*44*, *45*). These present studies suggest that MdmX and Mdm2:XZFRF, while clearly cytoplasmic, are also detected within the nucleus of cells lacking Mdm2 (Figure 4B). The cytoplasmic localization of Mdm2:XZFRF was somewhat surprising, given that this fusion possesses the Mdm2 NLS. Given the recent finding that DNA damage can affect the cellular localization of MdmX (*46*), it is possible that the MdmX zinc and ring finger domains altered the structure of this fusion to inhibit the Mdm2 NLS signal. We are presently examining how the localization of these fusions respond following cellular stress.

In H1299 cells, we examined whether the overexpression of the fusion proteins led to a stabilization of Hdm2 by exploring their colocalization with endogenous Hdm2 that was slightly induced by coexpression with p53 (Figure 5A) or at basal levels (Figure 5C). As predicted from the p53 ubiquitination results, the Mdm2:XZFRF was able to stabilize Hdm2, unlike the MdmX:2 fusions (Figure 5B). Taken together, these results suggest that the Mdm2:XZFRF shows a unique ability in H1299 cells to repress p53 transactivation by stabilizing endogenous Hdm2 thereby triggering an ubiquitin-mediated p53 degradation. This study reinforces the model that the MdmX ring finger domain lacks E3 ligase activity in vivo and that Mdm2 ubiquitination of p53 involves more than the Mdm2 E3 ligase domain within the ring finger.

ACKNOWLEDGMENT

We would like to thank Dr. Kadakia and members of the laboratory for their critical review of the manuscript.

REFERENCES

1. Hollstein, M., Sidransky, D., Vogelstein, B., and Harris, C. C. (1991) *Science 253*, 49−53.
2. Lakin, N. D., and Jackson, S. P. (1999) *Oncogene 18*, 7644−55.
3. Lane, D. P. (1992) *Nature 358*, 15−16.
4. Ko, L. J., and Prives, C. (1996) *Genes Dev. 10*, 1054−1072.
5. Levine, A. J. (1997) *Cell 88*, 323−331.
6. Cahilly-Snyder, L., Yang-Feng, T., Francke, U., and George, D. L. (1987) *Som. Cell Mol. Gen. 13*, 235−244.
7. Momand, J., Zambetti, G. P., Olson, D. C., George, D., and Levine, A. J. (1992) *Cell 69*, 1237−1245.
8. Oliner, J. D., Kinzler, D. W., Meltzer, P. S., George, D. L., and Vogelstein, B. (1992) *Nature 358*, 80−83.
9. Chen, J., Lin, J., and Levine, A. J. (1995) *Molec. Med. 1*, 142−152.
10. Honda, R., Tanaka, H., and Yasuda, H. (1997) *FEBS Lett. 420*, 25−27.
11. Honda, R., and Yasuda, H. (2000) *Oncogene 19*, 1473−1476.
12. Haupt, Y., Barak, Y., and Oren, M. (1996) *EMBO J. 15*, 1596−1606.
13. Kubbutat, M. H. G., Jones, S. N., and Vousden, K. H. (1997) *Nature 387*, 299−303.
14. Fuchs, S. Y., Adler, V., Buschmann, T., Wu, X., and Ronai, Z. (1998) *Oncogene 17*, 2543−2547.
15. Kubbutat, M. H., and Vousden, K. H. (1998) *Mol. Med. Today 4*, 250−256.
16. Momand, J., Wu, H. H., and Dasgupta, G. (2000) *Gene 242*, 15−29.

17. Shvart, A., Steegenga, W. T., Riteco, N., van Larr, T., Dekker, P., Bazuine, M., van Ham, R. C, van der Hoven van Oordt, V., Hateboer, G., van der Eb, A. J., and Jochemsen, A. G. (1996) *EMBO J. 15*, 5349−5357.
18. Jones, S. N., Roe, A. E., Donehower, L. A., and Bradley, A. (1995) *Nature 378*, 206−208.
19. Montes de Oca Luna, R., Wagner, D. S., and Lozano, G. (1995) *Nature 378*, 203−206.
20. Parant, J., Chavez-Reyes, A., Little, N. A., Yan, W., Reinke, V., Jochemsen, A. G., and Lozano, G. (2001) *Nat. Genet. 29*, 92−95.
21. Migliorini, D., Denchi, E. L., Danovi, D., Jochemsen, A., Capillo, M., Gobbi, A., Helin, K., Pelicci, P. G., and Marine, J. C. (2002) *Mol. Cell Biol. 22*, 5527−5538.
22. Finch, R. A., Donoviel, D. B., Potter, D., Shi, M., Fan, A., Freed, D. D., Wang, C. Y., Zambrowicz, B. P., Ramirez-Solis, R., Sands, A. T., and Zhang, N. (2002) *Cancer Res. 62*, 3221−3225.
23. Bottger, A., Bottger, V., Garcia-Echeverria, C., Chene, P., Hochkeppel, H.-K., Sampson, W., Ang, K., Howard, S. F., Picksley, S. M., and Lane, D. P. (1997) *J. Mol. Biol. 269*, 744−756.
24. Shvarts, A., Bazuine, M., Dekker, P., Ramos, Y. F. M., Steegenga, W. T., Merckx, G., van Ham, R. C. A., van der Houven van Oordt, W., van der Eb, A. J., and Jochemsen, A. G. (1997) *Genomics 43*, 34.
25. Jackson, M. W., and Berberich, S. J. (1999) *DNA Cell Biol. 18*, 693−700.
26. Jackson, M. W., and Berberich, S. J. (2000) *Mol. Cell. Biol. 20*, 1001−1007.
27. Stad, R., Ramos, Y. F., Little, N. A., Grivell, S., Attema, J., van der Eb, A. J., and Jochemsen, A. G. (2000) *J. Biol. Chem. 275*, 28039−28044.
28. Tanimura, S., Ohtsuka, S., Mitsui, K., Shirouzu, K., Yoshimura, A., and Ohtsubo, M. (1999) *FEBS Lett. 447*, 5−9.
29. Sharp, D. A., Kratowicz, S. A., Sank, M. J., and George, D. L. (1999) *J. Biol. Chem. 274*, 38189−38196.
30. Jackson, M. W., Lindstrom, M. S., and Berberich, S. J. (2001) *J. Biol. Chem. 276*, 25336−25341.
31. Berberich, S. J., Litteral, V., Mayo, L. D., Tabesh, D., and Morris, D. (1999) *Differentiation 64*, 205−212.
32. Xirodimas, D., Saville, M. K., Edling, C., Lane, D. P., and Lain, S. (2001) *Oncogene 20*, 4972−4983.
33. Haupt, Y., Maya, R., and Oren, M. (1997) *Nature 387*, 296−299.
34. Fang, S., Jensen, J. P., Ludwig, R. L., Vousden, K. H., and Weissman, A. M. (2000) *J. Biol. Chem. 275*, 8945−8951.
35. Oliner, J. D., Peitenol, J. A., Thiagalingam, S., Gyuris, J., Kinzler, K. W., and Vogelstein B. (1993) *Nature 362*, 857−860.
36. Kubbutat, M. H. G., Ludwig, R. L., Levine, A. J., and Vousden, K. H. (1999) *Cell Growth Differ. 10*, 87−92.
37. Stad, R., Little, N. A., Xirodimas, D. P., Frenk, R., van der Eb, A. J., Lane, D. P., Saville, M. K., and Jochemsen, A. G. (2001) *EMBO Rep. 2*, 1029−1034.
38. Thrower, J. S., Hoffman, L., Rechsteiner, M., and Pickart, C. M. (2000) *EMBO J. 19*, 94−102.
39. Argentini, M., Barboule, N., and Wasylyk, B. (2001) *Oncogene 20*, 1267−1275.
40. Bottger, V., Bottger, A., Garcia-Echeverria, C., Ramos, Y. F. M., van der Eb, A. J., Jochemsen, A. G., and Lane, D. P. (1999) *Oncogene 18*, 189−199.
41. Boyd, S. D., Tsai, K. Y., and Jacks, T. (2000) *Nat. Cell Biol. 2*, 563−568.
42. Geyer, R. K., Yu, Z. K., and Maki, C. G. (2000) *Nat. Cell Biol. 2*, 569−573.
43. Stommel, J. M., Marchenko, N. D., Jimenez, G. S., Moll, U. M., Hope, T. J., and Wahl, G. M. (1999) *EMBO J. 18*, 1660−1672.
44. Gu, J., Kawai, H., Nie, L., Kitao, H., Wiederschain, D., and Yuan, Z. M. (2002) *J. Biol. Chem. 277*, 19251−19254.
45. Migliorini, D., Danovi, D., Colombo, E., Carbone, R., Pelicci, P. G., and Marine, J. C. (2002) *J. Biol. Chem. 277*, 7318−7323.
46. Li, C., Chen, L., and Chen, J. (2002) *Mol. Cell Biol. 22*, 7562−7571.

BI0271291